

RECENT ARECIBO TIMING OF THE RELATIVISTIC BINARY PSR B1534+12

I. H. STAIRS

*University of Manchester, Nuffield Radio Astronomy Laboratories,
Jodrell Bank, Macclesfield, Cheshire, SK11 9DL, UK*

D. J. NICE, S. E. THORSETT, J. H. TAYLOR

*Joseph Henry Laboratories and Physics Department, Princeton University,
Princeton, NJ 08544 USA*

We present a new timing solution for PSR B1534+12, based on coherently-dedispersed observations at Jodrell Bank and, recently, Arecibo. The new data have resulted in improved measurements of the post-Keplerian timing parameters, including the orbital period derivative, \dot{P}_b . At present, the poorly-known distance to the pulsar limits the precision of the measurement of the intrinsic \dot{P}_b , and hence the strength of the test of general relativity that results from this binary system. By assuming that general relativity is the correct theory of gravity, we may invert the test and find an improved value of the pulsar distance.

1 Introduction

Double-neutron-star binary pulsars in close, highly eccentric orbits have long provided the best strong-field tests of the predictions of gravitational theories. The timing analysis of pulsar signals permits the measurement of five Keplerian orbital elements as well as a number of post-Keplerian (PK) orbital parameters. The PK parameters can be determined using a theory-independent procedure in which the masses of the two stars are the only unknowns.¹ Each of the PK parameters depends on the masses in a different way; consequently, if any two of them are measured, the relevant parameters of the two-body system are fully determined within any gravitational theory. If three or more PK parameters can be measured, a test of the gravitational theory results from the overdetermined system.

For the first binary pulsar, PSR B1913+16, the PK parameters $\dot{\omega}$ (rate of advance of periastron), γ (time dilation and gravitational redshift) and \dot{P}_b (orbital period derivative) have been measured and found to be in excellent agreement with the predictions of general relativity.^{2,3,4,5} PSR B1534+12, discovered in 1990,⁶ is a comparable system, with an eccentric 10.1-hour orbit. PSR B1534+12 is significantly brighter than PSR B1913+16, and its pulse profile has a narrow peak, permitting timing measurements of nearly five times greater accuracy. Because the orbit is nearly edge-on as viewed from the Earth, the PK parameters r and s (the “range” and “shape” of the Shapiro time delay) are measurable, in addition to $\dot{\omega}$, γ and \dot{P}_b . The resulting overtermination of the orbit leads to a non-radiative test of gravitation theory in the strong-field regime, complementing the $\dot{\omega}$ - γ - \dot{P}_b test for PSR B1913+16.⁷

Previously published timing measurements of PSR B1534+12 were made with the Arecibo 305 m telescope through early 1994,⁸ when the telescope went out of normal service for a major

upgrading; and from 1994 through 1997 with the 43 m telescope at Green Bank, West Virginia and the 76 m Lovell telescope at Jodrell Bank, England.⁹ With the recent reopening of Arecibo, we have been able to conduct a new series of observations of this pulsar in 1998 July, and improve on our previously reported timing results; in particular, we have reduced the uncertainty on the observed value of the PK parameter \dot{P}_b by 35%, to approximately 5% of the expected GR value.

2 Observations

A complete discussion of the observing procedures and instrumentation may be found in ref. 9. We only note here that over the years, new instrumentation was developed to remove more perfectly the pulse-smearing effects of interstellar dispersion. While the 1990-1994 Arecibo observations and the Green Bank observations used filterbanks to divide the observing bandpass into small channels, the later observations were carried out with an improved “coherent dedispersion” system, which sampled the raw telescope voltages and then removed the effects of dispersion using a software filter. The more recent observations therefore yield significantly better timing precision.

All observations involved folding the pulse signal over several minutes at the predicted topocentric pulse period to produce a total-intensity profile. Cross-correlation with a standard template, using a least-squares method in the Fourier transform domain, yielded a time offset.¹⁰ This offset was added to the time of the first sample of a period near the middle of the integration, thereby yielding an effective pulse arrival time. A different standard template was used for each observing system and frequency; they were made by averaging the available profiles over several hours or more. Uncertainties in the TOAs were estimated from the least squares procedure, and also from the observed scatter of the TOAs within 30 minutes of each one. Each observatory’s local time standard was corrected retroactively to the UTC timescale, using data from the Global Positioning System (GPS) satellites.

3 The Timing Model

A pulse received on Earth at topocentric time t is emitted at a time in the comoving pulsar frame given by

$$T = t - t_0 + \Delta_C - D/f^2 + \Delta_{R\odot} + \Delta_{E\odot} - \Delta_{S\odot} - \Delta_R - \Delta_E - \Delta_S. \quad (1)$$

Here t_0 is a reference epoch and Δ_C is the offset between the observatory master clock and the reference standard of terrestrial time. The dispersive delay is D/f^2 , where $D = \text{DM}/2.41 \times 10^{-4}$, with dispersion measure DM in cm^{-3}pc , radio frequency f in MHz, and the delay in seconds. Finally, $\Delta_{R\odot}$, $\Delta_{E\odot}$, and $\Delta_{S\odot}$ are propagation delays and relativistic time adjustments for effects within the solar system, and Δ_R , Δ_E and Δ_S are similar terms accounting for phenomena within the pulsar’s orbit.^{1,2,11} The orbital Δ terms are defined by:

$$\Delta_R = x \sin \omega (\cos u - e) + x(1 - e^2)^{1/2} \cos \omega \sin u, \quad (2)$$

$$\Delta_E = \gamma \sin u, \quad (3)$$

$$\Delta_S = -2r \ln \left\{ 1 - e \cos u - s \left[\sin \omega (\cos u - e) + (1 - e^2)^{1/2} \cos \omega \sin u \right] \right\}. \quad (4)$$

These are written in terms of the eccentric anomaly u and true anomaly $A_e(u)$, and the time dependence of ω , which are related by:

$$u - e \sin u = 2\pi \left[\left(\frac{T - T_0}{P_b} \right) - \frac{\dot{P}_b}{2} \left(\frac{T - T_0}{P_b} \right)^2 \right], \quad (5)$$

$$A_e(u) = 2 \arctan \left[\left(\frac{1+e}{1-e} \right)^{1/2} \tan \frac{u}{2} \right], \quad (6)$$

$$\omega = \omega_0 + \left(\frac{P_b \dot{\omega}}{2\pi} \right) A_e(u). \quad (7)$$

At a given time t , then, the propagation delay across the pulsar orbit is calculated by a model which incorporates ten parameters implicitly defined in the above equations: five Keplerian parameters (x, ω, T_0, P_b, e) and five PK parameters ($\dot{\omega}, \dot{P}_b, \gamma, r, s$). These quantities, in conjunction with a simple time polynomial to model the spin of the pulsar and with astrometric parameters to model the propagation of the signal across the solar system, constitute the free parameters to be fit in the theory-independent timing model.

In a particular theory of gravity, the five PK parameters can be written as functions of the pulsar and companion star masses, m_1 and m_2 , and the well-determined Keplerian parameters. In general relativity, the equations are^{1,2,11}

$$\dot{\omega} = 3 \left(\frac{P_b}{2\pi} \right)^{-5/3} (T_\odot M)^{2/3} (1 - e^2)^{-1}, \quad (8)$$

$$\gamma = e \left(\frac{P_b}{2\pi} \right)^{1/3} T_\odot^{2/3} M^{-4/3} m_2 (m_1 + 2m_2), \quad (9)$$

$$\dot{P}_b = -\frac{192\pi}{5} \left(\frac{P_b}{2\pi} \right)^{-5/3} \left(1 + \frac{73}{24}e^2 + \frac{37}{96}e^4 \right) (1 - e^2)^{-7/2} T_\odot^{5/3} m_1 m_2 M^{-1/3}, \quad (10)$$

$$r = T_\odot m_2, \quad (11)$$

$$s = x \left(\frac{P_b}{2\pi} \right)^{-2/3} T_\odot^{-1/3} M^{2/3} m_2^{-1}. \quad (12)$$

Here the masses m_1 , m_2 , and $M \equiv m_1 + m_2$ are expressed in solar units, and we use the additional shorthand notations $s \equiv \sin i$ and $T_\odot \equiv GM_\odot/c^3 = 4.925490947 \mu\text{s}$, where i is the angle between the orbital angular momentum and the line of sight, G the Newtonian constant of gravity, and c the speed of light.

4 Arrival Time Analysis

We used the standard TEMPO analysis software² together with the JPL DE200 solar-system ephemeris¹² to fit the measured pulse arrival times to the timing model with a least-squares technique. Arbitrary offsets were allowed between the different data sets to allow for frequency-dependent changes in pulse shape and slight differences in the standard profile alignments. To partially compensate for small systematic errors, uncertainties in TOAs were increased (in quadrature) by 2.9, 17.1, 20.5, 7.0, and 6.0 μs , respectively, when calculating weights for the 1990-94 Arecibo, Jodrell Bank, Green Bank data, 1998 Arecibo 430 MHz and 1998 Arecibo 1420 MHz sets.

Results for the astrometric, spin, and dispersion parameters of PSR B1534+12 are presented in Table 1. We fit the data to two models of the pulsar orbit. The theory-independent “DD” model¹¹ treats all five PK parameters defined in §3 as free parameters in the fit. Alternatively, the “DDGR” model^{2,13} assumes general relativity to be correct and uses equations 8 through 12 to link the PK parameters to $M \equiv m_1 + m_2$ and m_2 ; consequently it requires only two post-Keplerian free parameters.

Table 2 presents our adopted orbital parameters. Uncertainties given in the table are approximately twice the formal “ 1σ ” errors from the fit; we believe them to be conservative estimates of the true 68%-confidence uncertainties, including both random and systematic effects. The Keplerian orbital parameters include the period P_b , projected semi-major axis $x \equiv a_1 \sin i/c$,

Table 1: Astrometric, spin, and dispersion parameters for PSR B1534+12. Figures in parentheses are uncertainties in the last digits quoted, and italic numbers represent derived quantities.

Right ascension, α (J2000)	15 ^h 37 ^m 09 ^s .959952(16)
Declination, δ (J2000)	11° 55' 55".6561(3)
Proper motion in R.A., μ_α (mas yr ⁻¹)	1.5(2)
Proper motion in Dec., μ_δ (mas yr ⁻¹)	-25.6(3)
Parallax, π (mas)	< 1.5
Pulse period, P (ms)	37.9044404878550(14)
Period derivative, \dot{P} (10 ⁻¹⁸)	2.42250(3)
Epoch (MJD)	48778.0
Dispersion measure, DM (cm ⁻³ pc)	11.6152(16)
DM derivative (cm ⁻³ pc yr ⁻¹)	-0.00004(53)
Galactic longitude l (deg)	20.0
Galactic latitude b (deg)	47.8
Composite proper motion, μ (mas yr ⁻¹)	25.6(3)
Galactic position angle of μ (deg)	238.7(4)

eccentricity e , longitude of periastron ω , and time of periastron T_0 . These quantities are followed by the measured post-Keplerian parameters relevant to each of the two models. The DDGR solution includes a parameter called “excess \dot{P}_b ,” which accounts for an otherwise unmodeled acceleration resulting from galactic kinematics.

The best estimates of the masses of the pulsar and its companion come from the DDGR solution. We find the masses to be $m_1 = 1.344 \pm 0.002 M_\odot$ and $m_2 = 1.335 \pm 0.002 M_\odot$. For the sake of comparison Table 2 lists, in italic numbers, computed PK parameter values corresponding to the measured masses in the DDGR fit. The fitted and derived parameter values are in accord, indicating good agreement of the theory-independent solution with general relativity.

Figure 1 shows the post-fit residuals for the 1990–1994 Arecibo 1400 MHz data, the Jodrell Bank data, and the recent Arecibo 430 MHz data, plotted as functions of date. Even within a single data set, the TOA uncertainties can vary by factors of three or more because of scintillation-induced intensity variations. We have not attempted to show these differences in data quality by means of error bars in the residual plots.

5 Discussion

Before the observed \dot{P}_b can be compared to the theoretical value, we must apply a correction which accounts for the relative acceleration of the center-of-mass frame of the binary pulsar system and the solar system barycenter. An expression for the most significant bias, which arises from galactic kinematic effects, is derived in ref. 3. This bias can be written as the sum of terms arising from acceleration toward the plane of the Galaxy, acceleration within the plane of the Galaxy, and an apparent acceleration due to the proper motion of the binary system:

$$\left(\frac{\dot{P}_b}{P_b} \right)^{\text{gal}} = -\frac{a_z \sin b}{c} - \frac{v_0^2}{cR_0} \left[\cos l + \frac{\beta}{\sin^2 l + \beta^2} \right] + \mu^2 \frac{d}{c}. \quad (13)$$

Here a_z is the vertical component of galactic acceleration, l and b the galactic coordinates of the pulsar, R_0 and v_0 the Sun’s galactocentric distance and galactic circular velocity, μ and d

Table 2: Orbital parameters of PSR B1534+12 in the DD and DDGR models. Figures in parentheses are uncertainties in the last digits quoted, and italic numbers represent derived quantities.

	DD model	DDGR model
Orbital period, P_b (d)	0.42073729933(3)	0.42073729933(2)
Projected semi-major axis, x (s)	3.729464(3)	3.7294638(5)
Eccentricity, e	0.2736775(5)	0.2736774(2)
Longitude of periastron, ω (deg)	267.44738(10)	267.44744(9)
Epoch of periastron, T_0 (MJD)	48777.82595097(6)	48777.82595096(6)
Advance of periastron, $\dot{\omega}$ (deg yr $^{-1}$)	1.755794(19)	<i>1.75580</i>
Gravitational redshift, γ (ms)	2.071(6)	<i>2.067</i>
Orbital period derivative, $(\dot{P}_b)^{\text{obs}}$ (10 $^{-12}$)	-0.131(9)	<i>-0.1924</i>
Shape of Shapiro delay, s	0.983(8)	<i>0.9762</i>
Range of Shapiro delay, r (μ s)	6.3(1.3)	<i>6.6</i>
Total mass, $M = m_1 + m_2$ (M_\odot)		2.67845(4)
Companion mass, m_2 (M_\odot)		1.344(2)
Excess \dot{P}_b (10 $^{-12}$)		0.061(9)

the proper motion and distance of the pulsar; we use the short-hand notation $\beta = d/R_0 - \cos l$. The pulsar distance can be estimated from the dispersion measure, together with a smoothed-out model of the free electron distribution in the Galaxy.¹⁴ This model yields $d \approx 0.7$ kpc for PSR B1534+12, with an uncertainty of perhaps 0.2 kpc. At this distance we estimate $a_z/c = (1.60 \pm 0.13) \times 10^{-19}$ s $^{-1}$.¹⁵ Following ref. 3, we assume a flat galactic rotation curve and take $v_0 = v_1 = 222 \pm 20$ km s $^{-1}$ and $R_0 = 7.7 \pm 0.7$ kpc. Then, summing the terms in equation (13) and multiplying by P_b , we find the total kinematic correction to be

$$(\dot{P}_b)^{\text{gal}} = (0.038 \pm 0.012) \times 10^{-12}. \quad (14)$$

The uncertainty in this correction is dominated by the uncertainty in distance, which is only roughly estimated by the dispersion-measure model.

Our measurement of the intrinsic rate of orbital period decay is therefore

$$(\dot{P}_b)^{\text{obs}} - (\dot{P}_b)^{\text{gal}} = (-0.169 \pm 0.015) \times 10^{-12}. \quad (15)$$

Under general relativity, the orbital period decay due to gravitational radiation damping, $(\dot{P}_b)^{\text{GR}}$, can be predicted from the masses m_1 and m_2 (eq. 10), which in turn can be deduced from the high precision measurements of $\dot{\omega}$ and γ . The expected value is

$$(\dot{P}_b)^{\text{GR}} = -0.192 \times 10^{-12}. \quad (16)$$

Although the measured value in the pulsar center-of-mass frame differs from this prediction by 1.5 standard deviations, it can be brought into good agreement by increasing the pulsar distance to slightly over 1 kpc. Stated another way, we can assume that GR is the correct theory of gravity, measure the “excess \dot{P}_b ” for the system as described above and presented in Table 2, and then invert equation 13 to determine the pulsar distance.¹⁶ Figure 2 shows the relation between the two quantities; using this approach we obtain $d = 1.08 \pm 0.15$ kpc (68% confidence limit). The uncertainty is dominated by the measurement uncertainty of $(\dot{P}_b)^{\text{obs}}$, rather than uncertainties in the galactic rotation parameters or the acceleration a_z . Continued

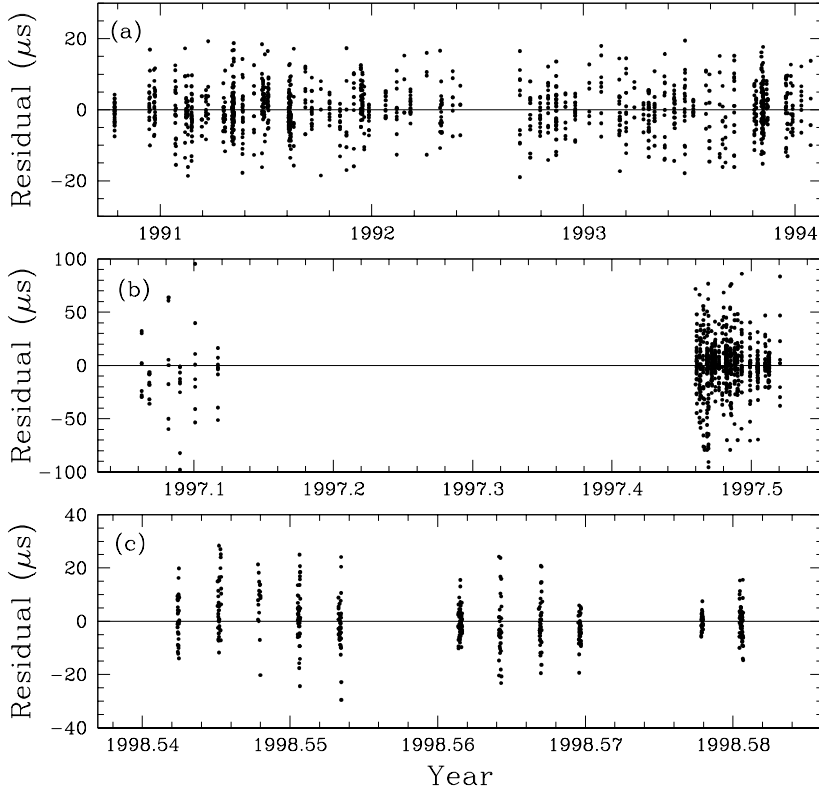


Figure 1: Post-fit residuals versus date for (a) Arecibo 1400 MHz, (b) Jodrell Bank and (c) Arecibo 430 MHz data.

timing of this system should lead to a much more precise distance measurement; in fact, the recent Arecibo observations have already reduced the uncertainty by 35% over our previously published value.⁹

We note that the timing solution provides a second, independent constraint on the distance. The upper limit on parallax, $\pi < 1.5$ mas (Table 1) constrains the distance to $d > 0.67$ kpc. While the parallax distance has less precision than the kinematic distance, it is reassuring that these measurements are in agreement.

An accurate distance for PSR B1534+12 is of considerable interest because this system, along with PSR B1913+16, is of prime importance in estimating the rate of coalescence of binary neutron-star pairs in a typical galaxy. Early estimates of the inspiral rate used much smaller distances for PSR B1534+12, including 0.4 kpc,¹⁷ 0.5 kpc,¹⁸ and 0.7 kpc,^{19,20} leading to a low estimate of its intrinsic luminosity. Our distance, compared to that estimated from the dispersion measure, increases the volume per B1534+12-type object by a factor of 2.5 to 4, depending on the unknown scale height of such systems in the Galaxy; this has helped lead to improved estimates of the neutron-star–neutron-star coalescence rate.^{9,21,22,23}

5.1 Test of Relativity

This pulsar provides the second test of general relativity based on the $\dot{\omega}$, γ , and \dot{P}_b parameters of a binary pulsar system, and is the first double-neutron-star binary to permit significant measurements of the Shapiro-delay parameters r and s . The left-hand sides of equations (8–12) represent measured quantities, as specified for this experiment in the “DD” column of Table 2.

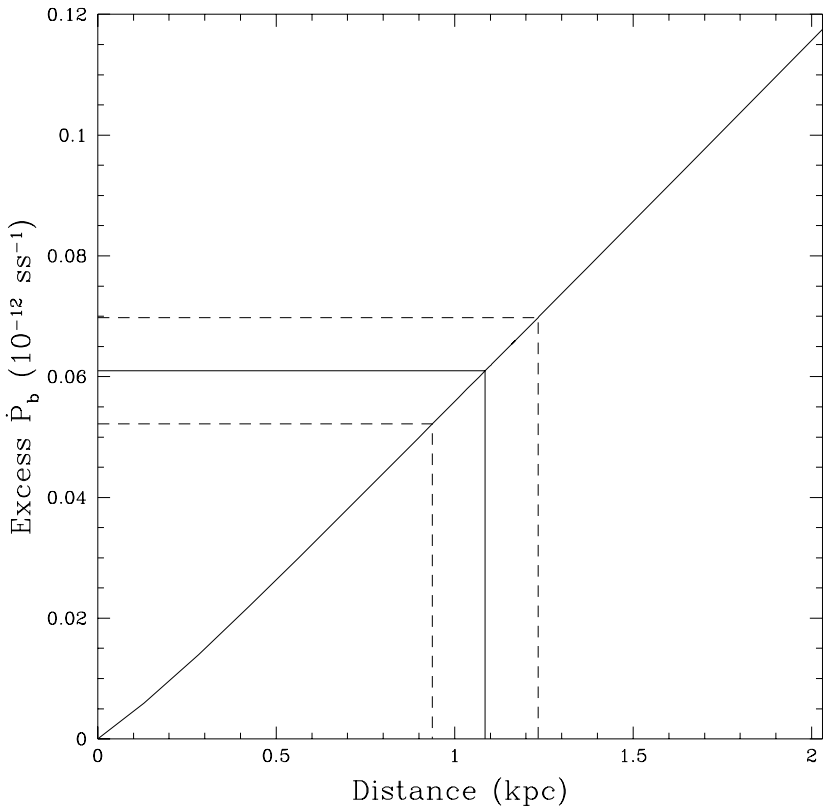


Figure 2: Relation between measured “excess \dot{P}_b ” and pulsar distance for the PSR B1534+12 system. Dashed lines indicate the 68% confidence ranges of the measured values.

If GR is consistent with the measurements and there are no significant unmodeled effects, we should expect the five curves corresponding to equations (8–12) to intersect at a single point in the m_1 - m_2 plane. A graphical summary of the situation for PSR B1534+12 is presented in Figure 3, in which a pair of lines delimit the 68% confidence limit for each PK parameter (a single line for $\dot{\omega}$, whose uncertainty is too small to show). A filled circle at $m_1 = 1.335 M_\odot$, $m_2 = 1.344 M_\odot$ marks the DDGR solution of Table 2, and its location on the $\dot{\omega}$ line agrees well with the measured DD values of γ and s . These three parameters therefore provide a unique test of the purely quasi-static regime of general relativity. We have already noted that the DD value of \dot{P}_b is slightly too small when corrected to the dispersion-estimated distance. However, as discussed above, this discrepancy can be removed by invoking a larger distance to the pulsar. Finally, the value of r , although presently little better than a 20% measurement, also agrees with its expected value. This pulsar thus provides a convincing second demonstration of the existence of gravitational radiation; furthermore, all its timing parameters are in good accord with general relativity theory.

Acknowledgments

The Arecibo Observatory, a facility of the National Astronomy and Ionosphere Center, is operated by Cornell University under a cooperative agreement with the National Science Foundation. The National Radio Astronomy Observatory is operated by Associated Universities, Inc., under a cooperative agreement with the US National Science Foundation. We thank Christopher Scafidi and Eric Splaver for assistance with observations. I. H. S. received support from NSERC

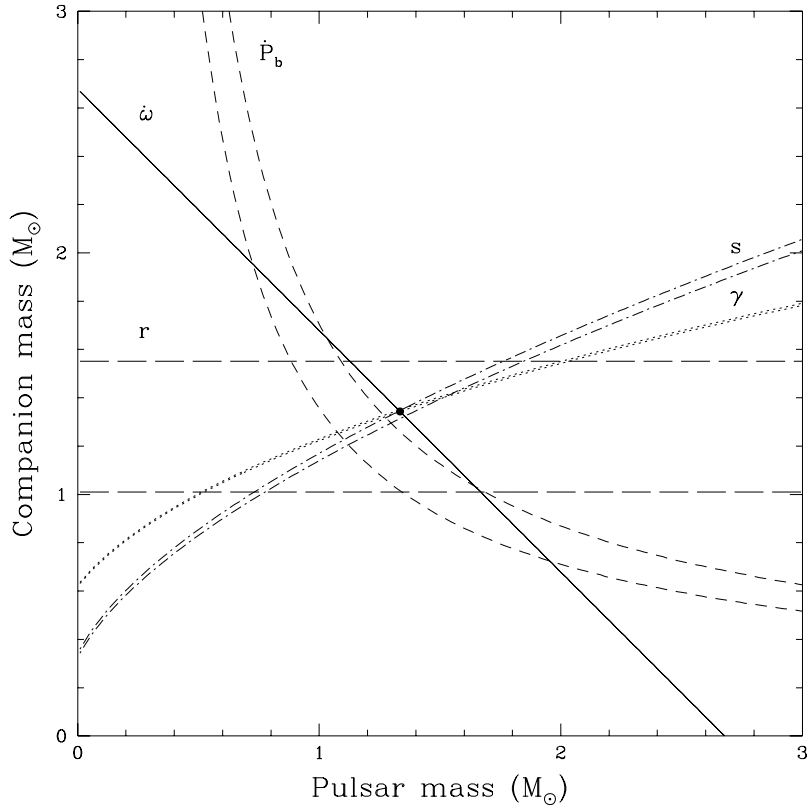


Figure 3: Mass-mass diagram for the PSR B1534+12 system. Labeled curves illustrate 68% confidence ranges of the DD parameters listed in Table 2. The filled circle denotes the component masses according to the DDGR solution. A kinematic correction for assumed distance $d = 0.7 \pm 0.2$ kpc has been subtracted from the observed value of \dot{P}_b . A slightly larger distance removes the small apparent discrepancy.

1967 and postdoctoral fellowships. S. E. T. is an Alfred P. Sloan Foundation Research Fellow.

References

1. T. Damour and J. H. Taylor. *Phys. Rev. D*, 45:1840–1868, 1992.
2. J. H. Taylor and J. M. Weisberg. *Astrophys. J.*, 345:434–450, 1989.
3. T. Damour and J. H. Taylor. *Astrophys. J.*, 366:501–511, 1991.
4. J. H. Taylor. *Reviews of Modern Physics*, 66:711–719, 1994.
5. J. H. Taylor. 1999. This volume.
6. A. Wolszczan. *Nature*, 350:688–690, 1991.
7. J. H. Taylor, A. Wolszczan, T. Damour, and J. M. Weisberg. *Nature*, 355:132–136, 1992.
8. Z. Arzoumanian. PhD thesis, Princeton University, 1995.
9. I. H. Stairs, Z. Arzoumanian, F. Camilo, A. G. Lyne, D. J. Nice, J. H. Taylor, S. E. Thorsett, and A. Wolszczan. *Astrophys. J.*, 505:352–357, 1998.
10. J. H. Taylor. *Phil. Trans. Roy. Soc. A*, 341:117–134, 1992.
11. T. Damour and N. Deruelle. *Ann. Inst. H. Poincaré (Physique Théorique)*, 44:263–292, 1986.
12. E. M. Standish. *Astr. Astrophys.*, 233:252–271, 1990.

13. J. H. Taylor. In M. A. H. MacCallum, editor, *General Relativity and Gravitation*, page 209, Cambridge, 1987. Cambridge University Press.
14. J. H. Taylor and J. M. Cordes. *Astrophys. J.*, 411:674–684, 1993.
15. K. Kuijken and G. Gilmore. *Mon. Not. R. astr. Soc.*, 239:571, 1989.
16. J. F. Bell and M. Bailes. *Astrophys. J.*, 456:L33–L36, 1996.
17. R. Narayan, T. Piran, and A. Shemi. *Astrophys. J.*, 379:L17–L20, 1991.
18. E. S. Phinney. *Astrophys. J.*, 380:L17–L21, 1991.
19. S. J. Curran and D. R. Lorimer. *Mon. Not. R. astr. Soc.*, 276:347–352, 1995.
20. E. P. J. van den Heuvel and D. R. Lorimer. *Mon. Not. R. astr. Soc.*, 283:L37–L39, 1996.
21. Z. Arzoumanian, J. M. Cordes, and I. Wasserman. *Astrophys. J.*, 1999. in press.
22. T. A. Prince. 1999. This volume.
23. V. Kalogera. 1999. This volume.